THE VOYAGER 1/SATURN ENCOUNTER AND THE COSMOGONIC SHADOW EFFECT

HANNES ALFVÉN

Dept. of Plasma Physics, Royal Institute of Technology, Sweden

and

Dept. of Applied Physics and Information Science, University of California, San Diego, La Jolla Calif., U.S.A.

(Received 15 April, 1981)

Abstract. If an electrically conducting medium (e.g. a dusty plasma) rotates around a gravitating central body, which possesses an axisymmetric dipole field, the medium is supported to two-thirds by the centrifugal force and to one-third by electromagnetic forces under the condition that the magnetic field is strong enough to controll the motion. If the electromagnetic forces disappear – e.g. by a de-ionisation of the dusty plasma – the medium will fall down to two-thirds of its original central distance. The result of this process will be a 'cosmogonic shadow effect' which is described in some detail.

The Voyager 1/Saturn results demonstrate that the macro-structure of the Saturnian ring system can be explained as a result of this effect working at the formation of the system. The agreement between the theoretical results and the observations is better than a few percent.

A similar analysis of the asteroidal belt shows that its macro-structure can also be explained by the cosmogonic shadow effect. The agreement between theory and observations is perhaps even better than in the Saturnian ring system.

The observational results demonstrate that during their formation both the Saturnian ring and the asteroidal belt passed a plasma state dominated by electromagnetic effects.

1. Early Theory of Cosmogonic Shadow

The first systematic attempt to base a theory of the origin of the solar system on electromagnetic or hydromagnetic effects was made in Alfvén (1942). The reason for doing so was that a basic difficulty with the old Laplacian hypothesis: how can a central body (Sun or planet) transfer angular momentum to the secondary bodies (planets or satellites) orbiting around it? It was demonstrated that this could be done by electromagnetic effects. No other acceptable mechanism has yet been worked out. An enormous literature based on the Laplacian (= non-hydromagnetic) approach to the origin of the solar system exists, but the basic Laplacian difficulty is still unsolved. Contrary to this, the electromagnetic transfer mechanism has been confirmed by observations, as described in the monograph *Cosmic Plasma* (Alfvén, 1981, pp. 28, 52, 53).

The hydromagnetic approach led to the discovery of two important *observational* regularities in the solar system: (1) the band structure, and (2) the cosmogonic shadow effect (the two-thirds fall down effect). Both have been discussed in detail in Alfvén and Arrhenius (1975, 1976). Further, the band structure has more recently been discussed by Alfvén (1981, p. 115). The second observational regularity, the cosmogonic shadow effect, will be the subject of this paper.

Astrophysics and Space Science **79** (1981) 491–505. 0004–640X/81/0792–0491$02.25.

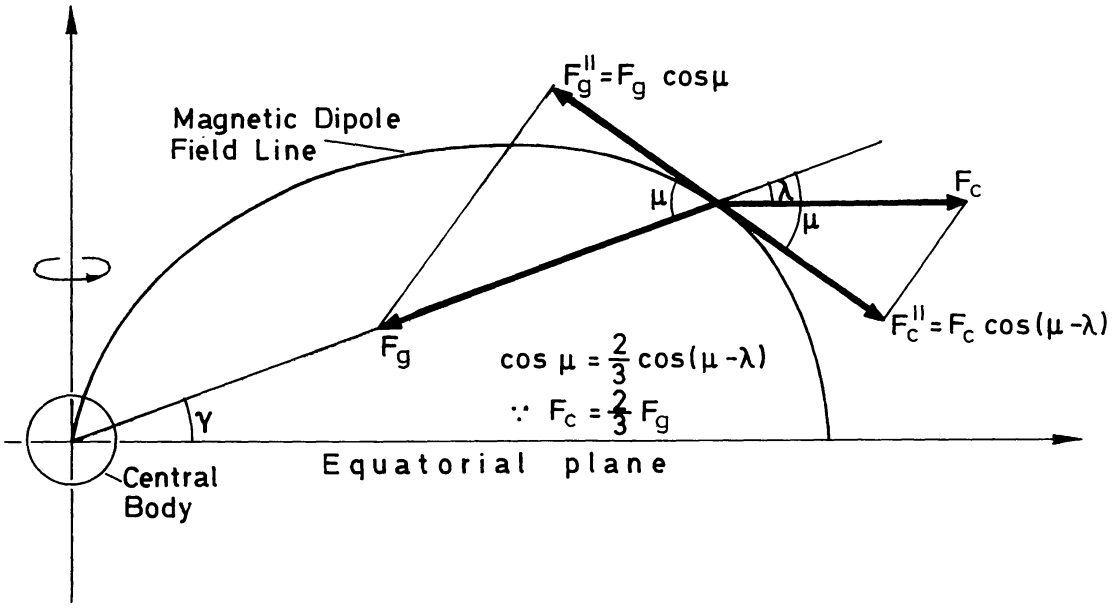

Fig. 1. Charged particles (electrons, ions, charged dust) in an axi-symmetric dipole field around a gravitating rotating body. If their motion is magnetic-field dominated, a quasi-stationary motion requires that the projections of gravitation and centrifugal force on the magnetic field line are equal. As shown by Alfvén and Arrhenius (1975, 1976) this means $v_\theta = (\frac{2}{3})^{1/2} v_K$, where v_θ is the rotational velocity and v_K the Kepler velocity.

The theoretical explanation of the two-thirds effect is very simple. If charged particles (electrons, ions or charged grains) move in a magnetic dipole field – strong enough to dominate their motion – under the action of gravitation and the centrifugal force, they will find an equilibrium in a circular orbit if their centrifugal force is $\frac{2}{3}$ of the gravitational force (Figure 1). The consequence of this is that if they become neutralized, so that electromagnetic forces disappear, the centrifugal force is too small to balance the gravitation. Their circular orbit changes to an elliptical orbit with the semi-major axis $a = \frac{3}{4}a_0$ and $e = \frac{1}{3}$ (where a_0 is the central distance where the neutralization takes place (Figure 2). Collisional (viscous) interaction between the condensed particles will eventually change the orbit into a new circular orbit with $a = \frac{2}{3}a_0$ and $e = 0$.

The two-thirds fall-down ratio leads to a 'cosmogonic shadow' effect. If, before the fall-down, there is plasma in the region $a_1 - a_2$, after the fall-down we will find matter in the region $\frac{2}{3}(a_1 - a_2)$. On the other hand, if the plasma in the region $a_2 - a_3$ is absorbed by a planet or satellite, or by small grains orbiting in that region, we will eventually find no (or very little) matter in the region $\frac{2}{3}(a_2 - a_3)$. In other words, matter in the region $a_2 - a_3$ will produce a *shadow* in the region $\frac{2}{3}(a_2 - a_3)$. As we shall see in this paper, this shadow effect can explain the macro-structure of the Saturnian rings (SR) and the main asteroidal region (AR). A more recent, but still pre-Voyager presentation is given by Alfvén (1976), and will be summarized in Figure 5.

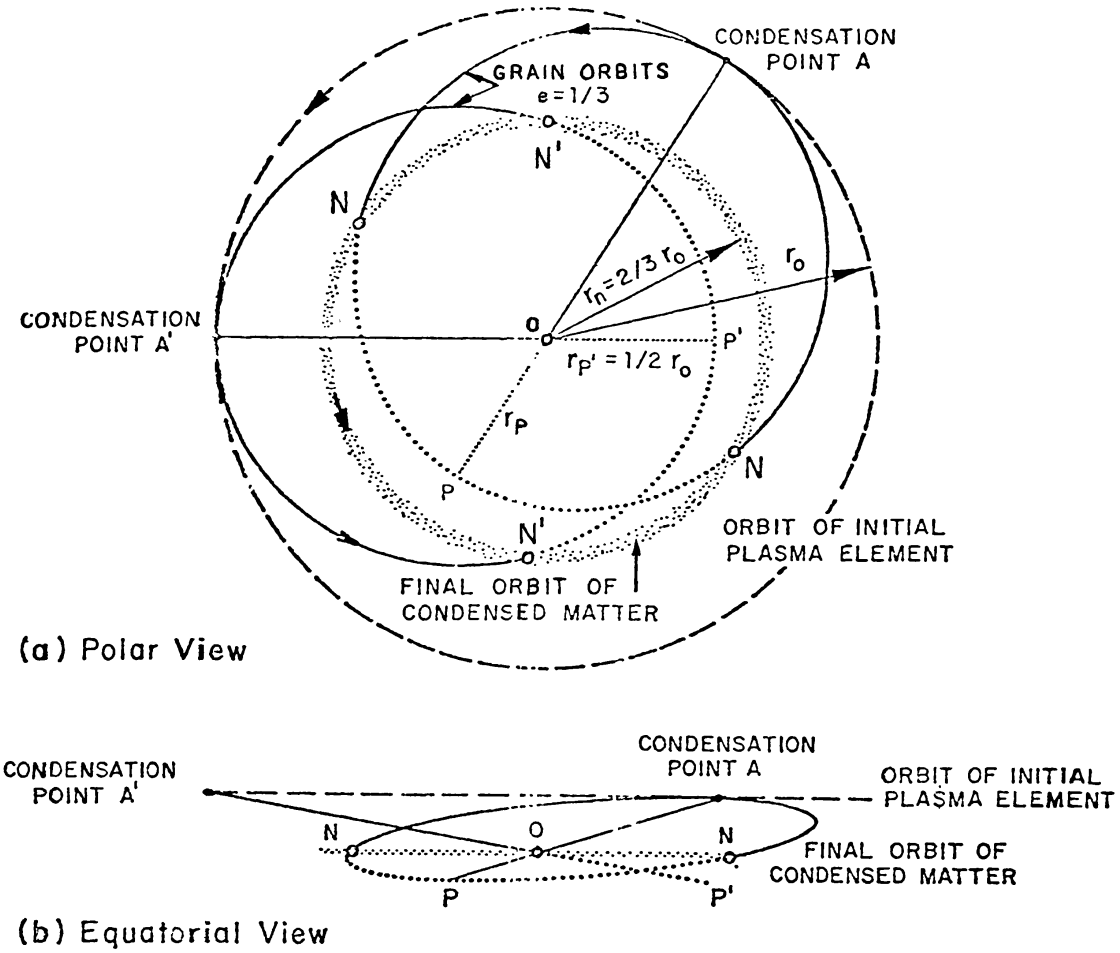

Fig. 2. Vanishing magnetic force give a transfer into elliptic orbits. If the magnetic field or the particle charge suddenly disappears, the particles at the central distance a_0 will orbit in ellipses with semi-major axis $a = \frac{3}{4}a_0$, and eccentricity $e = \frac{1}{3}$. They will collide mutually when they reach the nodes in the equatorial plane at $a = \frac{2}{3}$. Collisions will transform their orbits, eventually to circular orbits in the equatorial plane with $a = \frac{2}{3}a_0$, $e = 0$.

2. Correction of the Fall-Down Theory

When general interest in cosmic electrodynamics began to avalanche in the 1950's, it was thought appropriate to develop the cosmogonic theory further. A monograph on the origin of the solar system (Alfvén, 1954) was published. In this it was shown that in the SR, but not in the AR, the cosmogonic shadow produces a 'load' or 'reaction') on the particles producing the shadow, with the result that the ratio 2 : 3 = 0.67 should be reduced by about 5% (Figure 3). If the density function is approximated as $\rho = \text{const}\, a^n$, the reduction depends on the value of n. The value of n was estimated from the assumption that it was essentially the same in the whole region of the inner Saturnian satellite (ring–Rhea) and from this it was derived that the fall-down ratio should be reduced to $\Gamma = (\frac{2}{3})_{\text{corr}} = 0.63$–$0.65$ (Alfvén, 1954; p. 86–92).

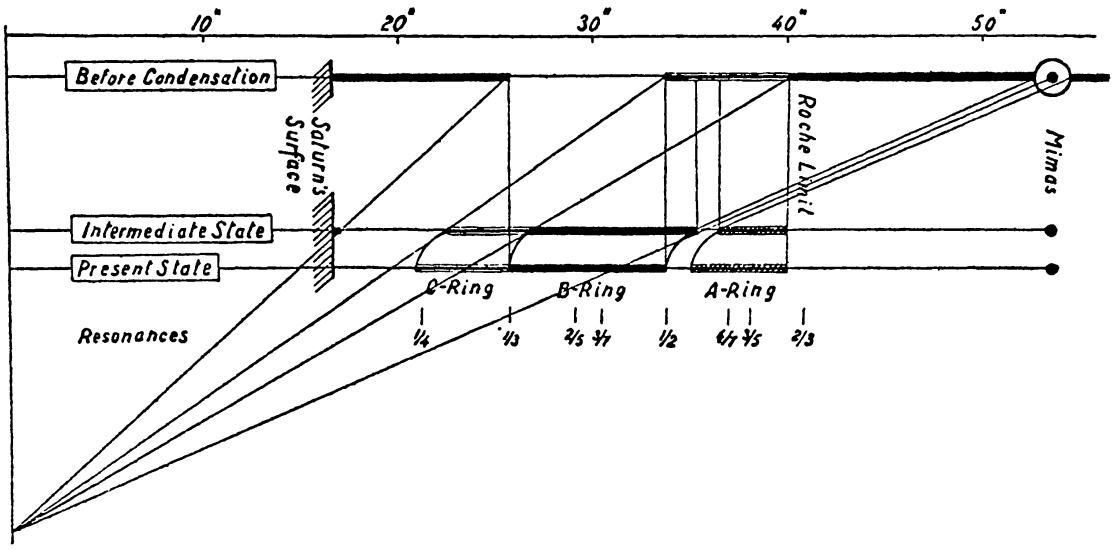

Fig. 3. Correction of the $\frac{2}{3}$– fall down ratio. The upper line, marked 'Before Condensation', shows the plasma density in the equatorial plane of Saturn, the center of which is at the left end. The next line, marked 'Intermediate State', represents the density of the grains produced by condensation of the gas. As these move at $\frac{2}{3}$– of the distance of the gas out of which they are produced, the density distribution is obtained by a geometrical construction reducing the central distances to $\frac{2}{3}$. The lower line, marked 'Present State', represents the density distribution into which the 'Intermediate State' is transformed by the 'shadow reaction', or 'shadow load'.

3. It is Reasonable that the present SR and AR Data are of Cosmological Relevance?

Before going into a detailed analysis of the observational results, it is necessary to clarify whether any present signatures in the SR and AR could in principle be fossils from cosmogonic times 4–5 $\times$ 10^9 yr ago. There are three reasons for not excluding this possibility.

(1) *The resonances* (with Jupiter in the AR and with Mimas, and possibly also other satellites in the SR) form a sort of obstacle blocking the free transfer of mass in the radial direction. This is especially conspicuous in the AR with the Kirkwood gaps, which are empty regions dividing the rings into a number of 'slices'. The ringlet structure of SR, according to the Voyager I reports, may to some extent support this conclusion.

(2) *The diffusion coefficient* of grains or planetesimals in Kepler orbits which collide inelastically is not positive (as in generally taken for granted) but *negative*, as shown by Baxter and Thompson (1971, 1973). This is illustrated by Figure 4. A positive diffusion coefficient would convert state A into B. But as already a qualitative discussion shows, inelastic collisions between the orbiting bodies will tend to smooth out the differences between their orbital parameters, so that the state B is transferred into A, which means a *negative* diffusion. The mathematical proof and the clarification of the circumstances under which this is true, are found in papers by Baxter and Thompson (1973, 1975). Their results may also explain the large number of 'ringlets' observed by Voyager I.

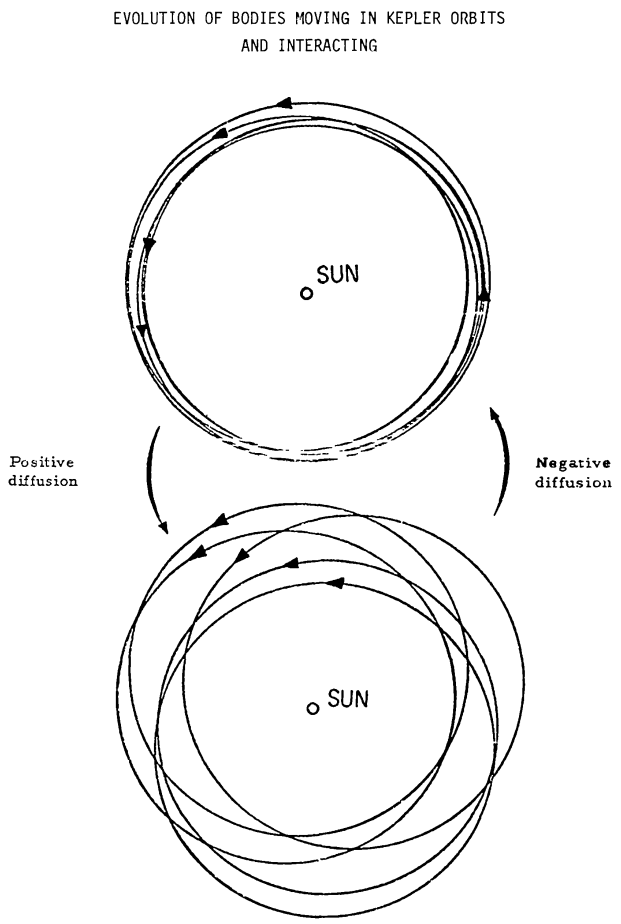

Fig. 4. Negative diffusion. If a number of grains or planetesimals orbit around a central body, as in the upper figure, collisions would change the orbits into the configuration shown in the lower figure if the diffusion were positive. In reality, collisions between the orbiting grains will tend to equalize their orbits, hence transforming the lower pattern into the upper (negative diffusion).

These may be analogous to the 'jet streams' which seem to be essential for the transfer of the planetesimal state into the present planet and satellite state.

(3) Other arguments are given by Alfvén and Arrhenius (1975, p. 163, and 1976, p. 311).

4. Pre-Voyager Results on Cosmogonic Shadow Effects in SR and AR

Before the Voyager 1/Saturn encounter, the best observations of the Saturnian rings were those of Dolfuss (1961, 1970) and Coupinot (1973). The state of the shadow effect in the light of these was summarized by Alfvén (1976). This paper also included a comparison with the AR.

The result of the latter is shown in Figure 5, which gives the *mass* density of the asteroidal belt as a function of *a*. Since the cosmogonic theory primarily refers to the *mass* distribution, it is essential to use this instead of the usual plot of the *number* as a

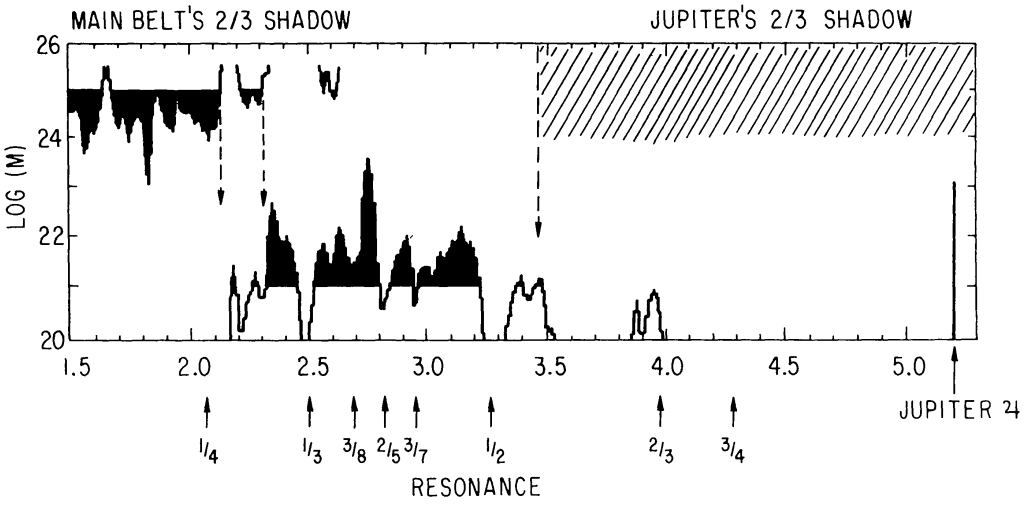

Fig. 5. Mass distribution in the asteroidal belt as a function of semi-major axis a. As the diagram is logarithmic, almost only the black areas count. Above is plotted the same diagram upside down and diminished by $\frac{2}{3}$ (Jupiter included). The Kirkwood gaps are marked. If their distortion of the cosmogonic effects is eliminated we find that the belt has a high density region between 3.22 and 2.36, and low density region up to 3.50 and down to 2.20. The inner limit of the high density region is $\frac{2}{3}$ of the beginning of the belt, and the inner limit of the whole belt is $\frac{2}{3}$ of the beginning of the high density region. See further Figures 9 and 10.

function of a. The mass is calculated from the absolute magnitude of each asteroid, assuming the density and albedo to be constant. As only the order of magnitude of the mass is essential, this approximation is legitimate.

The comparison with the expected cosmogonic shadow effect is made by introducing the same diagram (including the position of Jupiter) upside down and diminished in the ratio 2:3. In studying the diagram, it should be observed that the y-axis is logarithmic. Hence, to a first approximation, only the black areas count. The mass of the white areas represent less than 1%.

It is seen that in Jupiter's 'cosmogonic shadow' – i.e., outside $\frac{2}{3}$ of Jupiter's orbit, which means $a = 3.5$ – there is very little mass. Only the Hilda group at $a = 3.9$–4.0 represents any appreciable mass. (The Hilda group may be connected with the 3:2 resonance, and hence not directly relevant to our problem.)

The Kirkwood gaps which are resonance phenomena, dominate the fine structure of the belt. Indeed, the 2:1 and 3:1 resonances are very deep, and the 5:2 and 7:3 resonances are also conspicuous. The 2:1 resonance is the most pronounced depression, and may be the reason why the mass density in the belt does not reach its full value outside the gap. The most massive part of the belt begins at $a = 3.20$, immediately inside the 2:1 resonance, and continues until $a = 2.36$. Inside this limit, the average mass density (smoothing out the Kirkwood gaps) is smaller by about one order of magnitude. A sharp inner limit is located at 2.20. There are a number of small asteroids inside this limit, but their total mass is negligible. The same material will be presented in a somewhat different (and in some respects, in clearer form) in Figure 9.

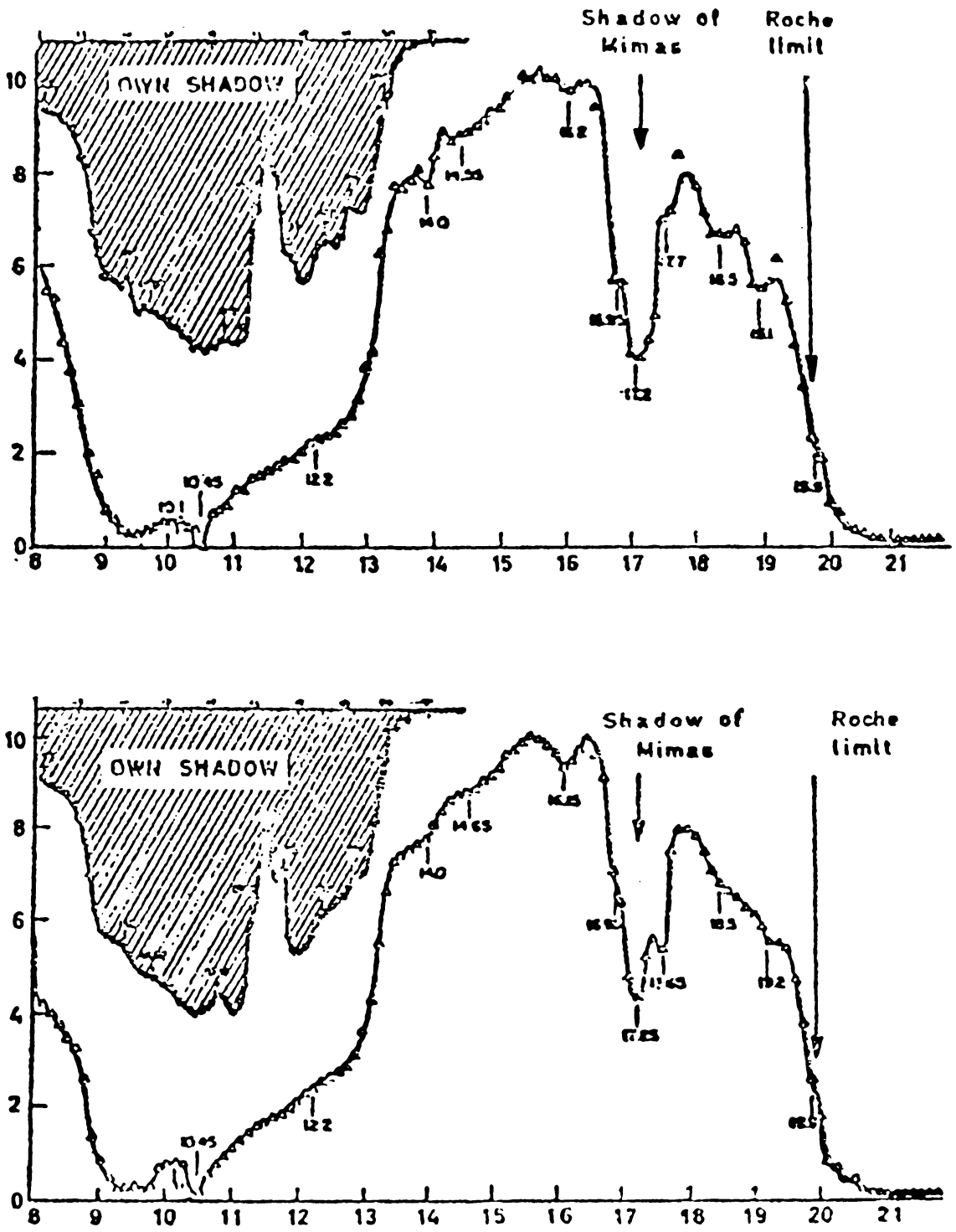

Fig. 6. Cosmogonic shadow effects explaining Coupinot's photometric diagrams of the Saturnian rings. The same treatment as in Figure 5 shows that Cassini's division is the cosmogonic shadow of Mimas, and the fall in intensity marking the border between the B and the C rings is the shadow of the Roche limit. See further Figure 10.

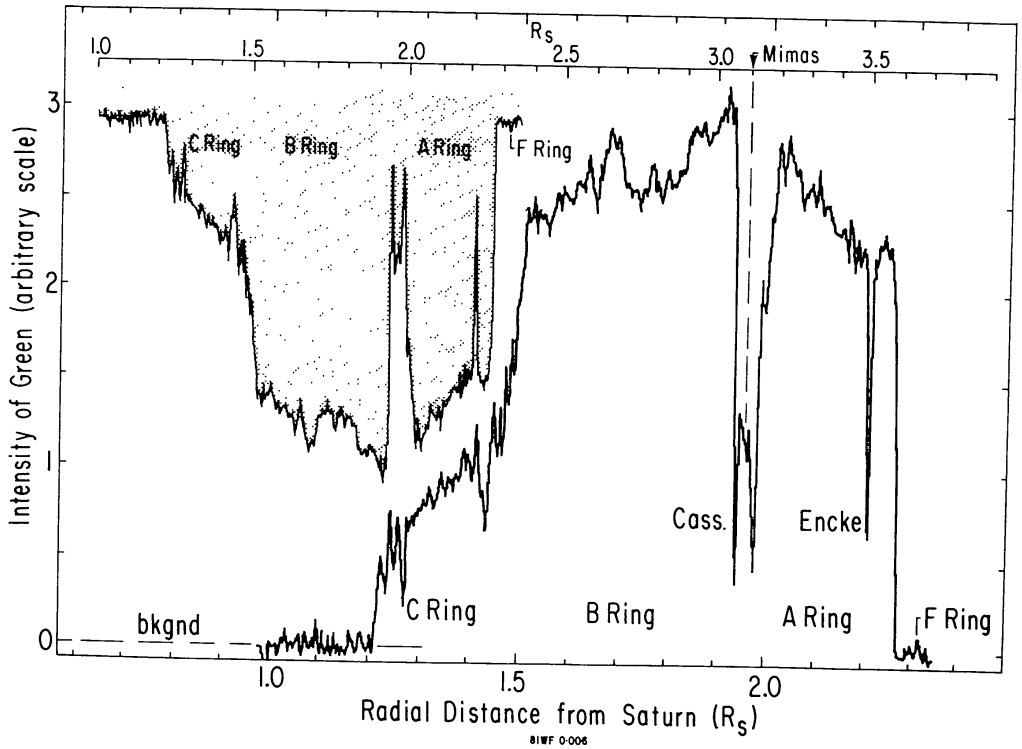

Fig. 7. Voyager 1/Saturn results. The same diagram as in Figure 6, but with the Voyager I/Saturn data. The fall down ratio is chosen to be 0.63. The results of the comparison are given in Table I.

TABLE I
Shadow effect in SR

	a	Γ
Mimas	3.10	
		0.63
Cassini center	1.96	
F-ring	2.33	
		0.63
Roche	2.26	
		0.65
Border B–C	1.48	
B outer	1.93	
		0.64
C inner	1.23	
Theoretical value		0.63–0.65

A similar diagram for the SR using two of Coupinot's photometric diagrams is seen in Figure 6. The shadow of Mimas gives the Cassini division and the beginning of the 'own' shadow of the SR explains the rather sharp fall in luminosity, marking the limit between the B and the C rings. The C ring data were not considered to be reliable.

5. The Voyager 1/Saturn Results

Figure 7 shows the photometric curve of the measurements in green, kindly placed at my disposal by Dr J. Cuzzi. The diagram also shows the cosmogonic shadow, as earlier obtained by reducing the size by a factor $\Gamma \simeq \frac{2}{3}$ and turning it upside down. Also, the orbital distance of Mimas is included. The exact value of Γ is somewhat uncertain. As stated in Section 2, it should be in the narrow range $0.63 < \Gamma < 0.65$. In order to place the shadow of Mimas exactly at the center of the Cassini division, the value of 0.63 has been chosen.

The diagram shows that the rapid decrease in intensity marking the border between the B and C rings coincides with the shadow of the Roche limit, just as in Coupinot's diagrams). But the more reliable data from the C ring *gives a new identification of a shadow effect:* the inner limit of the C ring, where the intensity drops to zero, is located where we expect the shadow of the outer limit of the B ring. This is logical, because it is not until we have passed the A ring and meet the B ring that the opacity of the ring system attains its full value.

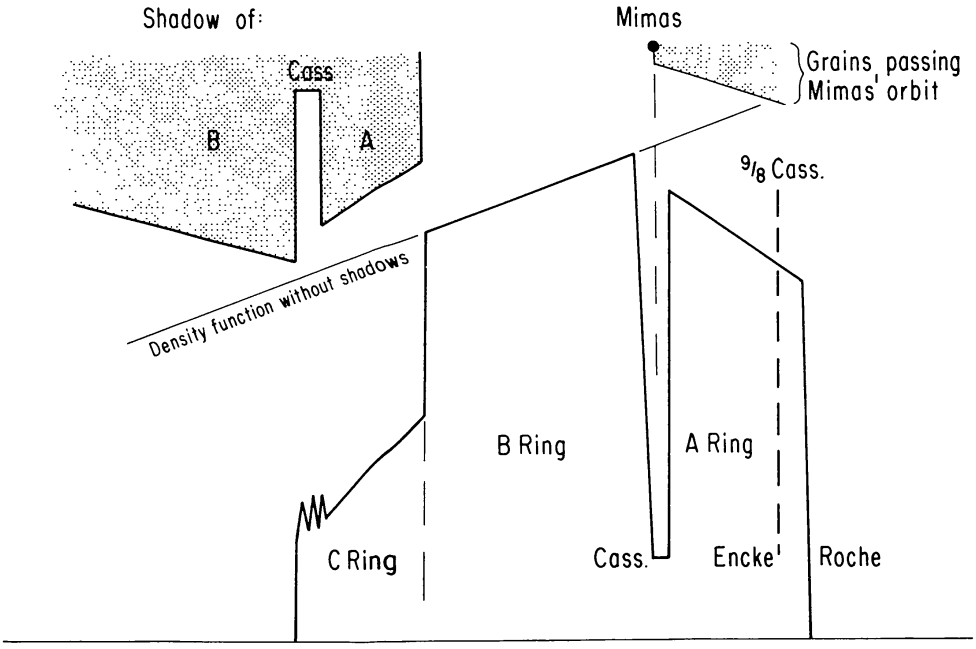

Fig. 8. Idealized picture of the Voyager 1/Saturn results. In order to concentrate the attention on the macro-structure, the micro-structure is smoothed out. Mimas produces the Cassini division, the Roche limit produces the fall in intensity between the B and C rings, and the outer edge of the B ring produces the inner limit to the C ring. If the center of Cassini is multiplied by 9:8, we reach the position of the Encke division.

The detailed results of the comparison are given in Table I. The value of Γ is 0.63 for Cassini-Mimas, and a slightly higher value is obtained for the outer B-inner C ratio. The B–C border is not very well defined. The luminosity drops from $a = 1.51$ to $a = 1.46$, with the steepest drop at $a = 1.49$. If this is compared with the rapid increase at the Roche limit at $a = 2.28$, we obtain $\Gamma = 0.65$. A comparison with the F ring at 2.33 gives $\Gamma = 0.63$. It is possible that the lack of sharpness at the transition is due to the combination of the Roche and F ring shadows.

Figure 8 shows an idealized picture of the observational curve (with all the small-scale features smoothed out for concentrating the attention on the large scale features. It is obvious that cosmogonic shadow effects can account for the main structure with the exception of the Encke division.

6. Details of the Transfer Mechanism from Ellipse to Circle

A particle in elliptic orbit has an *angular momentum* which equals that in a circular orbit $a = \frac{2}{3}a_0$, but its *energy* equals the energy that it would have in a circular orbit at $a = \frac{3}{4}a_0$. The orbiting grain may conserve its angular momentum C and reduce its energy by colliding inelastically with the ring particles. Indeed, if the grain originates from a point at some distance from the equatorial plane, it will not reach the equatorial plane until at the node, which is located at $a = \frac{2}{3}a_0$ (compare Figure 2). At this point it will hit already existing ring particles. Its impact velocity, in relation to the ring particles, has no angular velocity component because the grain has the same angular velocity as the ring particles it hits. Its radial component is $v_r = 0.29v_o$, where v_o is the orbital velocity of the ring particles. Moreover, it has a z-component depending upon how far from the equatorial plane it has condensed.

If the collision leads to a splitting of the impacting grain and perhaps also of the impacted ring particle, the fragments will either hit adjacent ring particles – which need not give very much spread in the momentum of the ring particles – or they may be ejected out in the region above (or below) the ring plane. The orbits of all these fragments are such that they will return to the ring plane at the other node, or – if they make no collisions there – they will return to the place where they originated. It is easily seen that this process will not necessarily produce an excessive spread in the value of the orbital momentum.

7. The Encke Division and the 9:8 Ratio

The Encke division was discovered more than a hundred years ago, but its existence had been questionable. The Voyager results clarify that this is because of its inordinate sharpness. It is unlikely that it is due to a resonance, because there is no obvious resonance to be expected there. Moreover, the resonance markings are usually not at all so deep. Its a-value 2.21 is 1.13 times the value of the center of the Cassini division.

This draws the attention to the possibility that the transition from the $a = \frac{3}{4}a_0$, $e = \frac{1}{3}$ orbit to a circular orbit may in principle occur also in an adiabatic way. This occurs if

the transfer is produced through the collision of a charged grain with magnetic inhomogeneities. A magnetic *field* produces a change in direction, but no change in energy of a *particle*. In principle, a transfer may also be produced by a succession of charging and discharging of the grain.

Without elaborating further on the details of such a process, we conclude that it will lead to a *circular orbit at* $a = \frac{3}{4}a_0$. As the position of this orbit will be changed due to the shadow load in the same way as the orbits at $a = \frac{2}{3}$, the least arbitrary way of checking the reality of such a mechanism is to take the ratio $\frac{3}{4}:\frac{2}{3} = \frac{9}{8}$.

Indeed, the observed ratio between the Encke and the (center of the Cassini division is 1.13, very close to $\frac{9}{8}$. From this we conclude that *the Encke division may be due to an adiabatic transfer from the original ellipse.*

8. Comparison with the Asteroidal Ring

The Voyager 1/Saturn results shall now be compared with AR density distribution. Figure 9 is essentially the same diagram as Figure 6, but the shadow diagram is removed and the material is represented in such a way as to make a quantitative

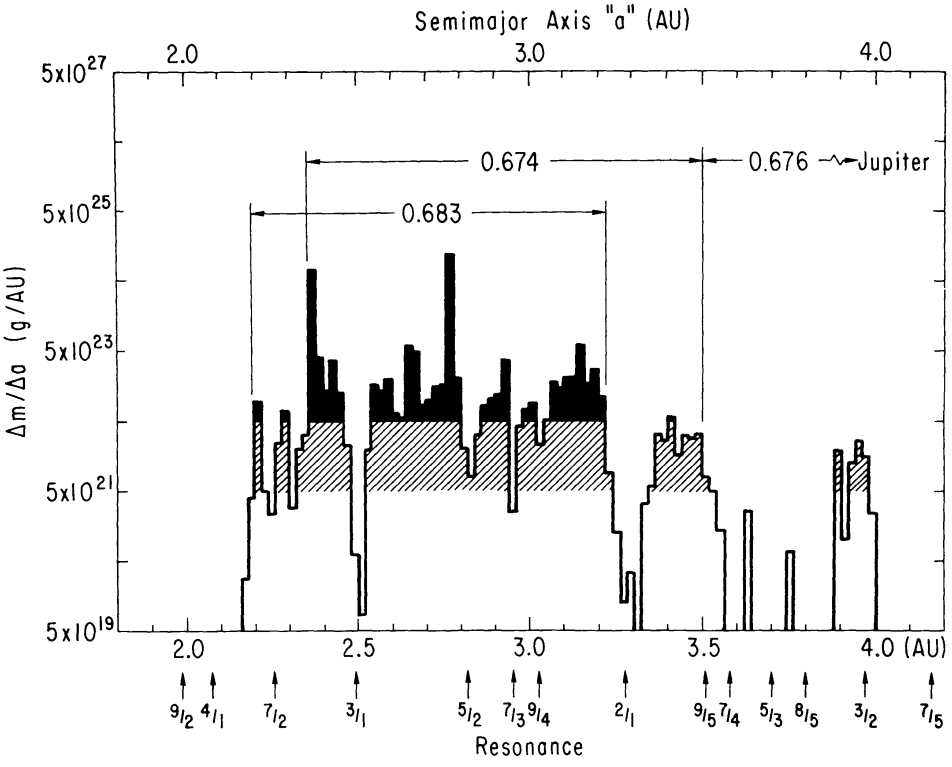

Fig. 9. Shadow effect in the AR. Essentially the same data as in Figure 6, but represented in such a way as to make the numerical comparison as accurate as possible. Note also that this diagram is logarithmic, so that to a first approximation only the black areas should be considered. The shaded areas represent one order of magnitude smaller mass density, and the white areas can be almost neglected. Results are summarized in Table II.

TABLE II
Shadow effect in AR

	a	Γ
Jupiter	5.18	
		0.676
Main belt outer limit	3.50	
		0.674
High density outer limit	3.22	
		0.683
High density inner limit	2.36	
Main belt inner limit	2.20	
Theoretical value		0.667

evaluation of Γ as accurate as possible. The black areas represent a mass density of about one order of magnitude larger than the shaded areas, and in the white areas the mass is negligible.

We can divide the AR into three parts:

(1) The high density AR, essentially *black*.

(2) The inner and outer rings of the main belt, essentially *shaded* regions.

(3) The Hilda band, which is *marginally shaded*.

As limits of these regions, we take the points where the rise or fall are steepest, as shown in Figure 9. The values of Γ, as defined in Section 2, are given in Table II.

As mentioned earlier, these values should theoretically be $2:3 = 0.667$, not corrected for shadow load (because this is taken up by the sub-visual asteroids which are likely to have a larger total cross-section than the visual asteroids).

Hence, the agreement between the observational and theoretical values is very good (discrepancies of only one or two percent).

9. Resonances

Figure 10 gives a comparison between the SR and AR, normalized to the orbital distances of Jupiter and Mimas, and with some of the main resonances with these bodies indicated.

The relation between resonances and shadow effects is most clearly shown in the AR. The Kirkwood gaps are very clearly marked and, hence, are easily distinguished from the shadow pattern. The very strong 2:1 resonance may be the cause of the low density of the outer ring, but this is far from certain. We do not yet have a clear reason for the low density of the main belt outside the 2:1 resonance. The 3:1 resonance is clearly shown and seems not to affect the average density which is essentially the same outside

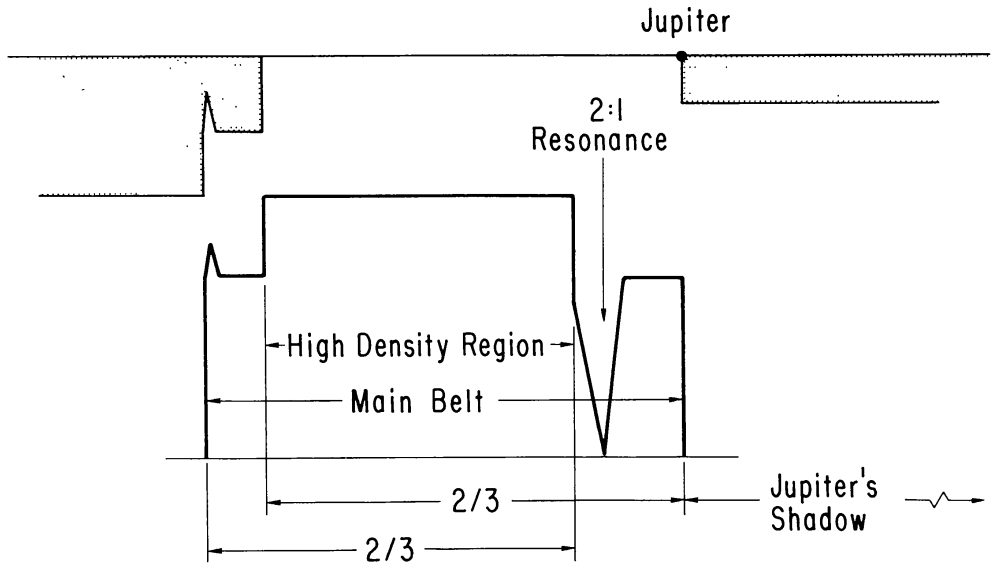

Fig. 10. Idealized picture of the AR with the Kirkwood gaps smoothed out.

as inside this resonance. The 4 : 1 resonance falls far below the inner limit (of the *mass* distribution, but there are numerous very small asteroids below this limit). The Hilda group has been attributed to the 3 : 2 resonance which falls in this region. In view of what has been found in the SR region, we should look for a 9 : 8 ratio in the AR region. We find that the ratio between the Hilda band and the outer edge of the main belt is close to 9 : 8. However, whether this is significant or not is not obvious.

The resonances in the SR are less easy to discuss. Earlier, the whole Cassini division has been attributed to the 2 : 1 resonance with Mimas, but this seems difficult to accept (Alfvén and Arrhenius, 1975, pp. 64, 66, 160–163; 1976, pp. 308–311). However, it seems likely that the inner edge of the Cassini division is sharpened by the 2 : 1 resonance. The 3 : 1 and 4 : 1 resonances fall close to the B–C border and the inner limit of the C ring. It seems unlikely that resonances can explain the macro-structure, but they are probably very important for the micro-structure. Further detailed study is necessary in order to clarify what effects are due to cosmogonic shadow, to resonances, and to other effects.

10. Discussion: Remarks on the Model

We have seen that the 1942 model (further developed in the 1954 model) can account for the macro-structure of the SR as found by Voyager I in 1980, with an accuracy of few percent. The agreement in the AR is perhaps even better. However, this does not necessarily mean that this old model, which has not been developed at all for a quarter of a century, is of a kind which can claim to be acceptable today. Indeed, our knowledge of cosmic plasma physics has changed so drastically during this time that this would be unreasonable.

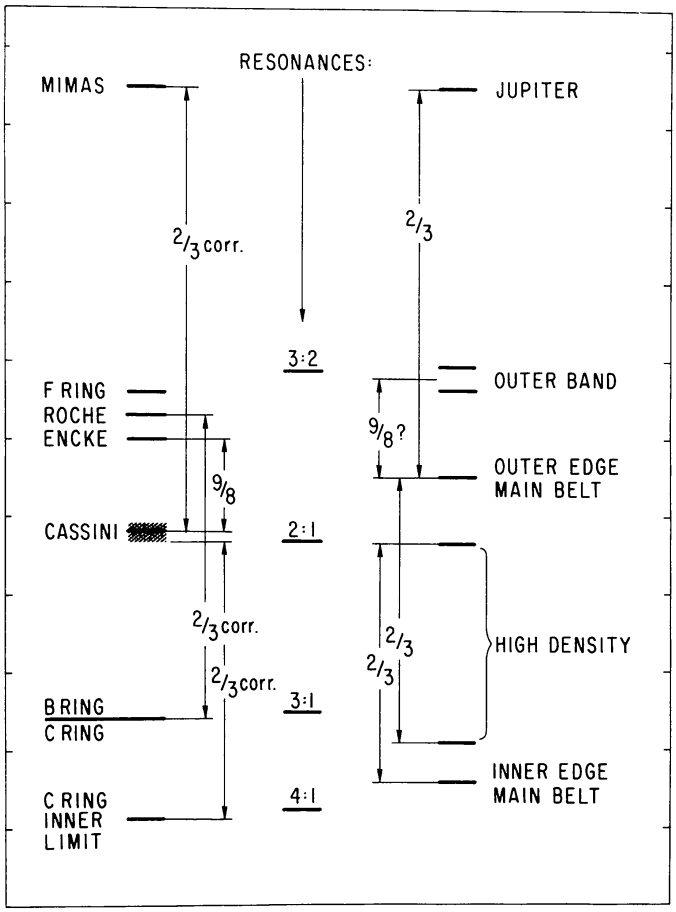

Fig. 11. Comparison between the Saturnian Ring and the Asteroid Region. Summary of the results of this paper, with the resonances plotted in the middle. In the AR the resonances are very pronounced (Kirkwood gaps) but there is no obvious connection with the smoothed out macro-structure, except that the high density main belt begins close below the 2:1 resonance. Whether the outer band (the Hilda's) are due to a 3:2 resonance or are 9:8 of the outer edge of the belt (or both!) is an open question.

Because of the very small mass of Mimas, the macro-structure of SR is probably not produced by resonances at all. However the 3:1 and 4:1 resonances fall close to the B–C limit and inner limit of C ring, and the resonance effects should be studied more closely. The 2:1 resonance probably sharpens the inner limit of Cassini.

Of special importance is that like all models of these times, the old model is essentially *homogeneous*, and the rather thorough revision of cosmic plasma physics which is under way now (cf., Alfvén, 1981) implies that it probably has to be replaced by an inhomogeneous model.

Hence the theoretical problem we are facing is to work out a more general model, which is similar to the old model in the respect that a $\frac{2}{3}$ fall-down ratio can be derived from it. This seems quite possible to do. If the result should be that the model works only if essential parameters (like density, degree of ionization, magnetic field, etc.,) are within certain limits, then the observational fall-down ratios will allow us to conclude that at the time when the SR and AR were formed, the parameters were within these

limits in these regions. This may give us an important criterion for checking the viability of different cosmogonic theories.

Acknowledgments

I wish to thank Dr J Cuzzi for placing his measurements of the Saturnian rings at my disposal and Dr D. Soderblom for clarifying discussions about the Voyager 1/Saturn results. I also thank Dr Walker Fillius and Dr Jay Hill, who have kindly helped me with the analysis of the data, Dr G. Arrhenius and Dr A. Mendis for important discussion, Mrs. Pat Gifford for preparing the figures, and Mrs Jane Chamberlin for the editing.

References

Alfvén, H.: 1942, *Stockholms Observatoriums Annaler* **14,** No. 2.
Alfvén, H.: 1954, *On the Origin of the Solar System*, Clarendon Press, Oxford.
Alfvén, H.: 1976, *Astrophys. Space Sci.* **43,** 97.
Alfvén, H.: 1981, *Cosmic Plasma*, D. Reidel Publ. Co., Dordrecht, Holland.
Alfvén, H. and Arrhenius, G.: 1975, *Structure and Evolutionary History of the Solar System*, D. Reidel Publ. Co., Dordrecht, Holland.
Alfvén, H. and Arrhenius, G.: 1976, *Evolution of the Solar System*, NASA SP–345, Washington, D.C.
Baxter, D. and Thompson, W.: 1971, in T. Gehrels (ed.), *Physical Studies of Minor Planets*, NASA SP–267, Washington, D.C., p. 319.
Baxter, D. and Thompson, W.: 1973, *Astrophys. J.* **183,** 323.
Coupinot, G.: 1973, *Icarus* **19,** 212.
Dollfus, A.: 1961, in G. P. Kuiper and B. M. Middlehurst (eds.), *The Solar System*, Vol, 3, Chicago, p. 568.
Dollfus, A.: 1970, *Icarus* **11,** 101.